We are IntechOpen, the world's leading publisher of Open Access books Built by scientists, for scientists

4,800
Open access books available

122,000
International authors and editors

135M
Downloads

Our authors are among the

154
Countries delivered to

TOP 1%
most cited scientists

12.2%
Contributors from top 500 universities

CLARIVATE ANALYTICS BOOK CITATION INDEX INDEXED

WEB OF SCIENCE™

Selection of our books indexed in the Book Citation Index in Web of Science™ Core Collection (BKCI)

Interested in publishing with us?
Contact book.department@intechopen.com

Numbers displayed above are based on latest data collected.
For more information visit www.intechopen.com

18

Finite element analysis on v-die bending process

Sutasn Thipprakmas
King Mongkut's University of Technology Thonburi
Thailand

1. Introduction

Bending is a common metalworking process used in sheet-metal forming to fabricate curve-shaped products of various sizes, such as parts of automobiles, aircraft, and ships shown in Fig. 1(a), in addition to various consumer products, such as kitchenware and sanitary products, depicted in Fig. 1(b).

(a) Automobile product (b) Consumer product

Fig. 1. Examples of bent products

The bending process is based on engineering science and has a large variety of applications. In addition, bending also features in many sheet metal–forming processes, such as the deep drawing and stamping processes sketched in Fig. 2.

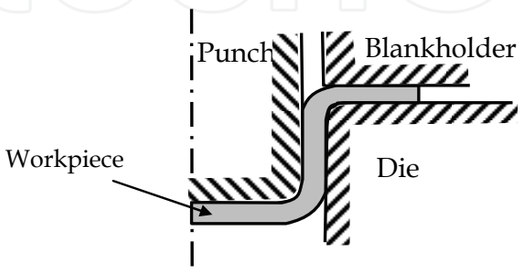

Fig. 2. Bending in deep-drawing process

According to DIN 8586, the bending process is subdivided into two groups as follows:
(1) Bending by using a linear die motion, in which the tool moves linearly to bend the workpiece; for example, the wiping-die bending and U-die bending processes, shown in Fig. 3(a).
(2) Bending by using a rotating die motion, in which a tool moves in rotations to bend the workpiece, as shown in Fig. 3(b). The basic advantages of rotary bending are less bending-force requirement, elimination of the use of a blankholder, and a final bending angle greater than 90 degree.

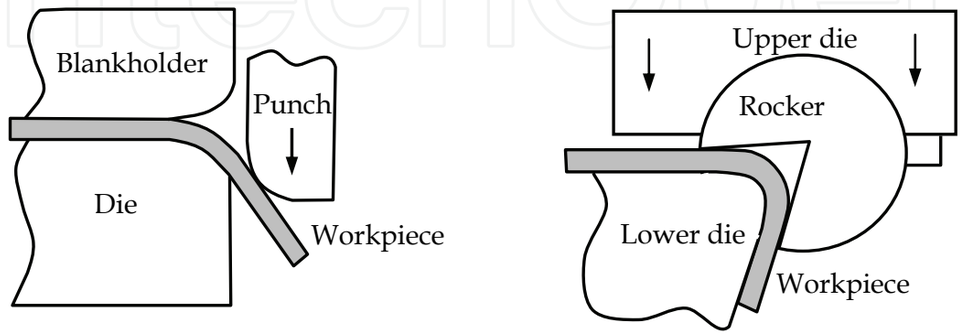

(a) Linear die motion (b) Rotating die motion

Fig. 3. Classification of bending process according to DIN 8586

Bending is a manufacturing process by which a force, corresponding to a given punch displacement, acts on the workpiece. The workpiece is initially bent in an elastic region. As the process continues, the workpiece is deformed by plastic deformation, thereby changing its shape. In the bending process, the bending load increases until the elastic limit of the material is exceeded. The material state enters the plastic deformation region and sheet metal can be formed. Specifically, the stress generated in the workpiece is greater than the yield strength but lower than the ultimate tensile strength of the material. The workpiece initially deforms where the bending moment is the greatest. For example, in the case of the V-die bending process, the process of permanent deformation starts directly underneath the punch. During the bending operation, the outer surface of the workpiece generates the greatest stretch, which then propagates inward toward the neutral plane. Similarly, the inner surface of the workpiece generates the greatest compression, which also then propagates inward toward the neutral plane. These distributions of the stresses are represented in Fig. 4.
This bending process results in formation of both a crack that usually occurs on the outer surface and a wrinkle that usually occurs on the inner surface. In addition to these crack and wrinkle defects, the major problem in the bending process is the accuracy of the part, including the part's geometry and dimension. These problems are directly influenced by the parameters of the bending process, such as properties and thickness of the material, angle and radius of bending, and the bending stroke (Schuler, 1998), (Lange, 1985). These problems were investigated in many earlier researches, where the finite element method (FEM) and related experimental protocols were conducted. The sequence of sheet-metal bending was optimized using a robot (Shigeru & Atsushi, 2002).

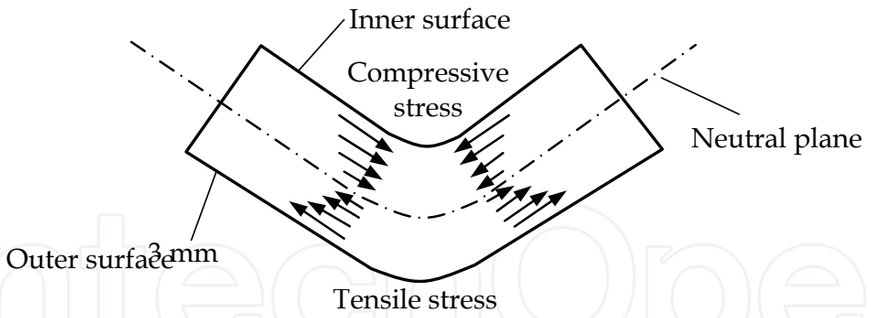

Fig. 4. Stress distribution in the V-die bending process

The plastic collapse of aluminum extrusions in biaxial bending was investigated (Belingardi & Peroni, 2007). The spring-back deformation during bending of a tube was studied (Da-xin et al., 2009). The deformation behavior of a thin-walled tube in rotary-draw bending under push assistant–loading conditions was investigated (Li et al., 2010). The modeling of the inelastic bending of a metal sheet was studied by applying thermal coupling was studied (Woznica & Klepaczko, 2003). The bending moment and spring-back was studied in the pure bending of anisotropic sheets (Alexandrov & Hwang, 2009). The process of sheet-metal bending was investigated using computer-aided techniques (Duflou et al., 2005). A thermomechanical model was identified for air bending (Canteli et al., 2008). The influence of the coining force on spring-back reduction in a V-die bending process was investigated (Leu & Hsieh, 2008). The spring-back in wiping–die bending processes was examined by applying both an experimental approach and the response surface methodology (Mkaddem & Saidane, 2007). The air bending and spring-back of stainless steel–clad aluminum sheets was studied (Yilamu, et al., 2010). The bending of thin sheets of stainless steel was studied by a raster-scanned low-power CO_2 laser (Vsquez-Ojeda & Ramos-Grez, 2009). The modeling of spring-back, strain rate, and Bauschinger effects for the two-dimensional steady-state cyclic flow of sheet metal subjected to bending under tension was investigated (Sanchez, 2009).

Most of the previous research works studied the spring-back phenomenon, including the effects of process parameters on it. Therefore, in this chapter, the spring-go phenomenon has been investigated thoroughly and will be discussed in depth. It will also serve as the basis for theoretically explaining the spring-go phenomenon that occurs during the bending process in comparison to the spring-back phenomenon. In addition, the effects of process parameters, including the radius and height of the punch, have been investigated and will be clearly discussed. Next, the spring-back and spring-go phenomena, including the effects of the punch radius and punch height, were investigated using the FEM; the FEM simulation results were also validated by experiments. On the basis of material-flow and stress-distribution analyses, the FEM simulation results showed that both spring-back and spring-go phenomena, in addition to the effects of punch radius and punch height, could be theoretically elucidated. In addition, the FEM simulation results also showed the possibility of using the FEM to predict spring-back and spring-go characteristics.

2. Principle of V-die Bending Process

The V-die bending process is the bending of a V-shaped part in a single die. The principle of the V-die bending process is shown in Fig. 5. The workpiece is bent between a V-shaped punch and die. The force acting on the punch causes punch displacement and then the workpiece is bent. The workpiece is initially bent as an elastic deformation. With continued downward motion by the punch, plastic deformation sets in when the stresses exceed the elastic limit. This plastic deformation starts on the outer and inner surfaces directly underneath the punch. The greatest tensile stress is generated on the outer surface, whereas the greatest compressive stress is generated on the inner surface; these stresses decreasingly propagate inward toward the workpiece. Therefore, crack formation usually occurs on the outer surface and a wrinkle usually occurs on the inner surface. The initial bending stage—the so-called "Air bending"—starts the moment the punch establishes contact with the workpiece and is completed either when the legs of the workpiece become tangential to the faces of the die or when the smallest internal radius of the workpiece becomes smaller than the radius of the punch. As the process continues, after completion of air bending, the bending is focused on the three points of the punch and the two faces of the die. The contact points between the workpiece and die are shifted toward the centerline of the die, and the legs of the workpiece try to close around the punch. As the punch proceeds further, the legs of the workpiece establish contact with the punch, and it is pressed to open up again until the bend angle approaches the die angle (Schuler, 1998), (Lange, 1985). The clearance between the punch and the die in V-die bending is commonly dependent of the workpiece thickness. The usual thickness of the workpiece in the V-die bending process ranges from approximately 0.5 to 25 mm.

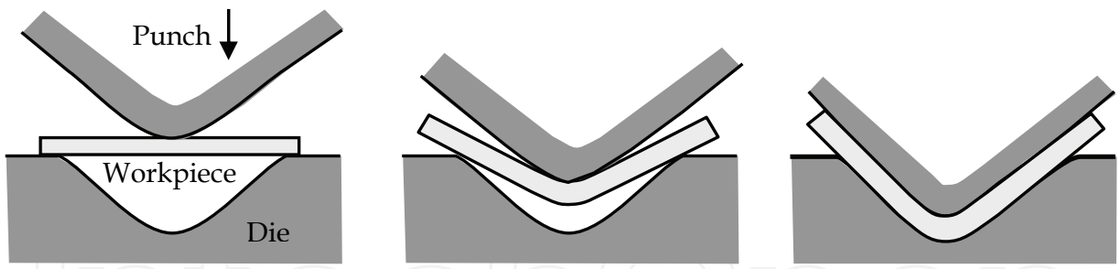

(a) Initial state (b) Bending state (c) Final state

Fig. 5. Principle of the V-die Bending Process

3. Classification of V-die Bending Process

The basic advantages of the V-die bending process are as follows:
(1) a simple tool design,
(2) an economical setup time, and
(3) an enormous range of sizes and complex shapes that can be fabricated for the part.

Therefore, the V-die bending process is generally used in both the Press Brake machine and the Press machine associated with press-form tooling. However, the basic disadvantage of

the use of the Press Brake machine is low productivity. The Press Brake machine is suitable for production of only a small quantity or the prototype of a product.
In addition to the classification of the V-die bending process based on the Press machine, the V-die bending process can be classified into two categories, namely, partial and full V-bending, as depicted in Fig. 6. Partial V-die bending (Fig. 6a) uses a V-bending punch containing a punch smaller than the workpiece; thus, it cannot establish contact with the whole surface of the workpiece on the die side. In Fig. 6(b), a full V-die bending is shown, where the workpiece completely establishes contact with the surfaces on both sides of the punch and die.

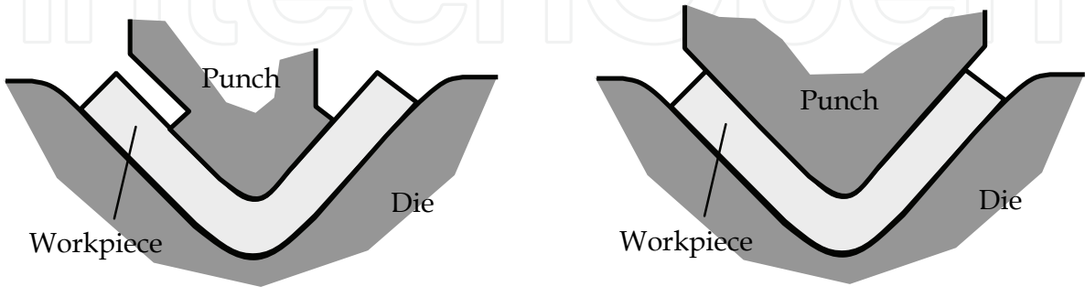

(a) Partial V-die bending (b) Full V-die bending

Fig. 6. Classification of the V-die Bending Process

4. Problems in V-die bending process

Considering the accuracy of the produced part, the product in the sheet metal–forming process is set higher requirements consisting of precise dimensions. These consist of fundamentally the same requirements as for the V-die bending process. Unwanted deformation generally occurs in the bending zone (underneath the punch), especially, the thick part of the workpiece and sharp bends, which results in a decrease in the accuracy of the part, as sketched in Fig. 7.

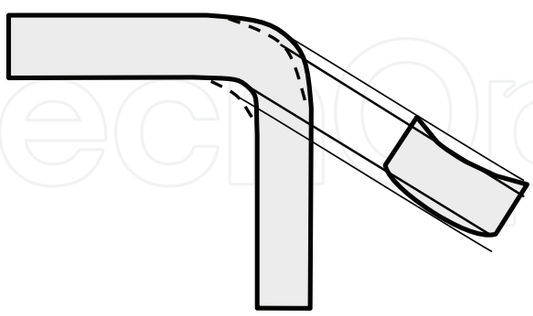

Fig. 7. Unwanted Deformation of the Cross Section during Bending

During the bending process, sufficient material flow to replace the material displaced is ensured to prevent the weakening and fracturing taking place at the workpiece corners (Schuler, 1998), (Lange, 1985). In addition, achieving the desired bend angle is very difficult and is the major problem in the bending process, especially in mass production. The reason is the occurrence of spring-back or spring-go feature. This problem is the key factor that

decreases the quality of the bent part. In addition, in practice, applying control over the spring-back or spring-go feature is very difficult because this feature is dependent on many process parameters, such as the material property, material thickness, and the angle, radius, and stroke of bending (Schuler, 1998), (Lange, 1985). Many earlier researches have investigated the spring-back and spring-go features to resolve these two in the bending process that is applied in many industrial problems by using the FEM and related experiments. The spring-back of CK67 steel sheet in V-die and U-die bending processes was investigated (Bakhshi-Jooybari et al., 2009). The spring-back control of sheet-metal air-bending process was studied (Wang et al., 2008). The variation of elastic modulus during plastic deformation and its influence on spring-back was investigated (Yu, 2009). The spring-back in the wipe-bending process of sheet metal was investigated using a neural network (Kazan et al., 2009). The spring-back of stainless steel sheet metal in V-bending dies was determined (Tekaslan et al., 2008). The spring-back prediction, compensation, and optimization were investigated using numerical analysis (Meinders et al., 2008). The spring-back characteristics of aluminum sheet–metal alloys under warm forming conditions were investigated using the numerical method (Kim & Koc, 2008). The spring-back and spring-go phenomena were investigated using the FEM (Thipprakmas & Rojananan, 2008). The spring-back in the bending of aluminum sheets was investigated using the FEM (East et al., 2002). The impact of physical parameters on spring-back appearance in U-draw bending was investigated by using FEM (Papeleux et al., 2002). The process parameters, such as die clearance, die radius, and step height, and their effects on spring-back were studied using the FEM (Ling et al., 2005). The amount of spring-back in steel sheet–metal of 0.5-mm thickness in a bending die was investigated (Tekaslan et al., 2006). The spring-back in sheet-metal bending was investigated using FEM (Panthi et al., 2007). The amount of spring-back on the spring material was investigated using FEM (Jin et al., 2000). The effects of punch height in partial V-bending process were investigated (Thipprakmas, 2010).

As mentioned above, the principle of the V-die bending is not very difficult to understand; however, a great degree of expertise and skills are required as this is an important technique for increasing the productivity and for improving product quality. Therefore, the characteristic features of bending must be theoretically understood. In addition, the effects of the process parameters related to the geometry and properties of the material must be strictly considered to achieve high-quality bent parts. To fully understand this process, the characteristic features of bending and the effects of the process parameters will be completely dealt with through theoretical investigation and explanation in this chapter.

5. Mechanism of Spring-back Phenomenon

According to the plastic deformation theory, the material is generally divided into two zones: the elastic and the plastic zones. The elastic property tries to maintain the material in the initial shape, whereas the plastic property tries to retain the material in the deformed shape. In the sheet metal–bending process, the bending load increases until the elastic limit of the material is exceeded and then the material state enters the plastic deformation zone. The outer surface of the material generates the tensile stress, which propagates inward toward the neutral plane. Vice versa, the inner surface of the material generates the compressive stress and it propagates inward toward the neutral plane. Because of the stress distributions, this phenomenon causes the formation of a small elastic band around the

neutral plane, as shown in Fig. 8. As the bending force is removed at the end of the bending stroke, the inner surface–generated compressive stress tries to enlarge the workpiece and the outer surface–generated tensile stress tries to shrink. In contrast, the elastic band remains in the bent parts trying to maintain its original shape, resulting in a partial recovery toward its initial shape. This elastic recovery is called "spring-back". Thus, the workpiece tries to spring back and the bent part slightly opens out, as shown in Fig. 9.

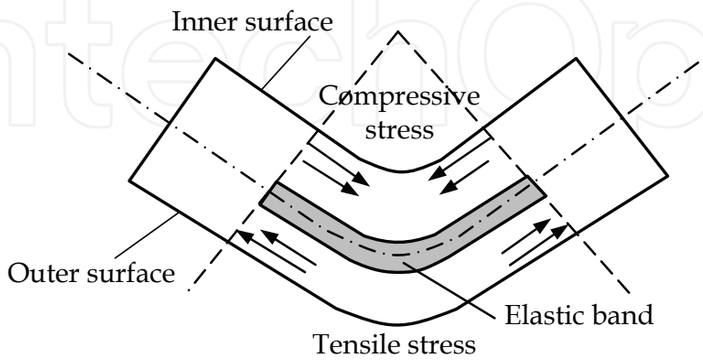

Fig. 8. Illustration of the Elastic Band in the Bent Part

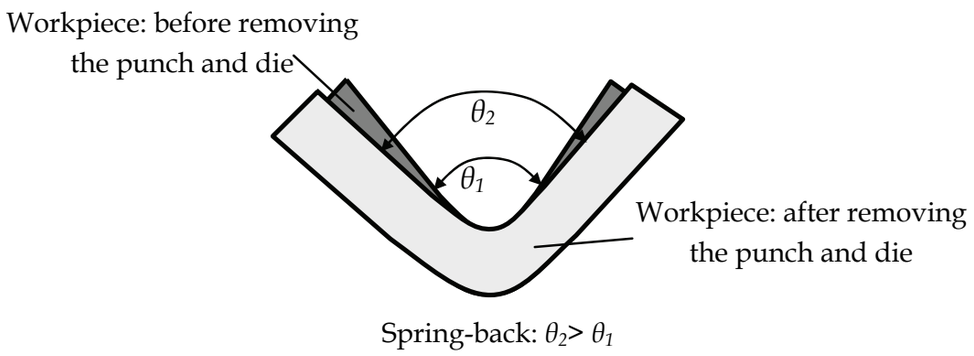

Fig. 9. Illustration of Spring-back Feature

6. Mechanism of Spring-go Phenomenon

In addition to the spring-back feature, the spring-go feature usually occurs in a bending process. The spring-back characteristic occurs as the bent part slightly opens. In contrast, the spring-go characteristic occurs as the bent part slightly closes, as shown in Fig. 10.

The concept of the spring-go phenomenon has rarely been theoretically clarified in previous researches. However, the spring-go phenomenon was investigated in the author's previous researches. FEM simulation was used as a tool for investigating and understanding the theoretical basis of the spring-go phenomenon. The FEM-simulation model used in the previous study by the current author is shown in Fig. 11.

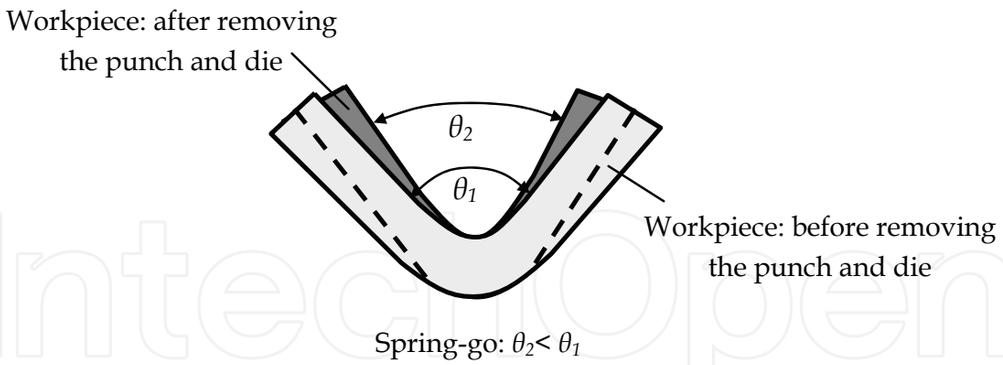

Fig. 10. Illustration of Spring-go Feature

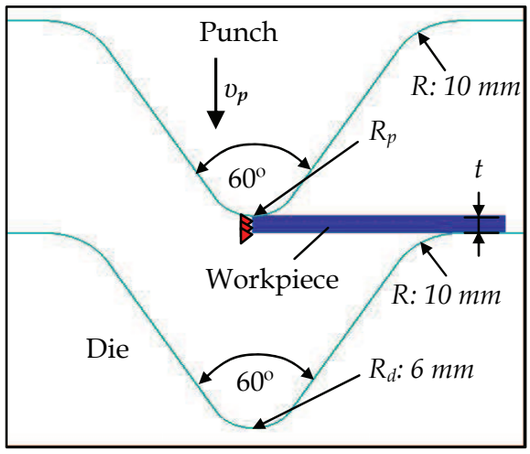

Fig. 11. FEM-Simulation Model

Simulation model	Plane strain model
Object type	Workpiece : Elasto-plastic Punch/Die : Rigid
Bended material	A1100-O (σ_B=92.5MPa, λ=46%) (t= 3mm, length 70 mm)
Friction coefficient (μ)	0.1
Flow curve equation	$\bar{\sigma} = 160.4\bar{\varepsilon}^{0.22}$
Die radius (R_d)	6 mm
Angular punch radii (R_p)	1, 2, 3, 4, 5, 6 mm
Punch height (H_p)	6, 16, 26, 36 mm
Bending angle (θ)	60°
Punch velocity (υ_p)	0.05 mm/sec

Table. 1. FEM-Simulation Conditions and Material Property

The two-dimensional plane strain with a simulation model of 35-mm length and 3-mm thickness was investigated. The commercial analytical code (DEFORM-2D) for a two-dimensional implicit quasi static FEM was used as the FEM-simulation tool. The workpiece material was aluminum A1100-O (JIS), which was set as an elasto-plastic type, with the rectangular meshes consisting of approximately 3500 elements. The punch and die were set as rigid type. Table 1 shows the details of the FEM-simulation conditions and the material properties. Similar to the results of previous research, on the basis of the material-flow analysis and stress distribution, the spring-go phenomenon has been investigated thoroughly and will be discussed in depth compared with the spring-back phenomenon.

6.1 Material-Flow Analysis

Referring to the author's previous research (Thipprakmas & Rojananan, 2008), Fig. 12 shows the FEM simulation analysis of the material flow feature in the workpiece with reference to the punch radius. The FEM simulation results showed the same feature of material flow during a small bending stroke, as shown in Fig. 12(a-1), (b-1), and (c-1). Specifically, the material was allowed to flow into the die along the punch direction. As the punch proceeded further, before the workpiece contacted the sides of the punch, as the punch radius decreased, both the velocity of the leg of the workpiece (zone A) and the gaps at the zones B and C increased, as shown in Fig. 12(a-2), (b-2), and (c-2).

After the workpiece contacted the side of the punch, as shown in Fig. 12(a-3), (b-3), and (c-3), the workpiece was pushed backward toward the die, resulting in an S-curve-shaped material-flow characteristic; therefore, a reverse-bending feature was generated. It was observed that the punch could proceed further as the punch radius decreased. Before removing the punch, in the case of small punch radii as shown in Fig. 12(a-4), the punch pressed the workpiece so that the latter was in contact with the die corner, whereas the leg of the workpiece had not yet completely contacted the side of the die. Therefore, an S-curve-shaped material-flow feature was generated. In contrast, the punch radius increased as shown in Fig. 12(b-4) and (c-4), the leg of the workpiece was already in contact with the die's side and therefore, the punch cannot push the workpiece into the die corner, resulting in a gap between the workpiece and the die (zone D). Therefore, the S-curved feature of the material flow was reduced; the S-curved material flow decreased as the punch radius was increased. Importantly, this S-curved material flow affected the stress distribution, resulting in the reversed bending characteristic; therefore, the required bending angle could not be achieved.

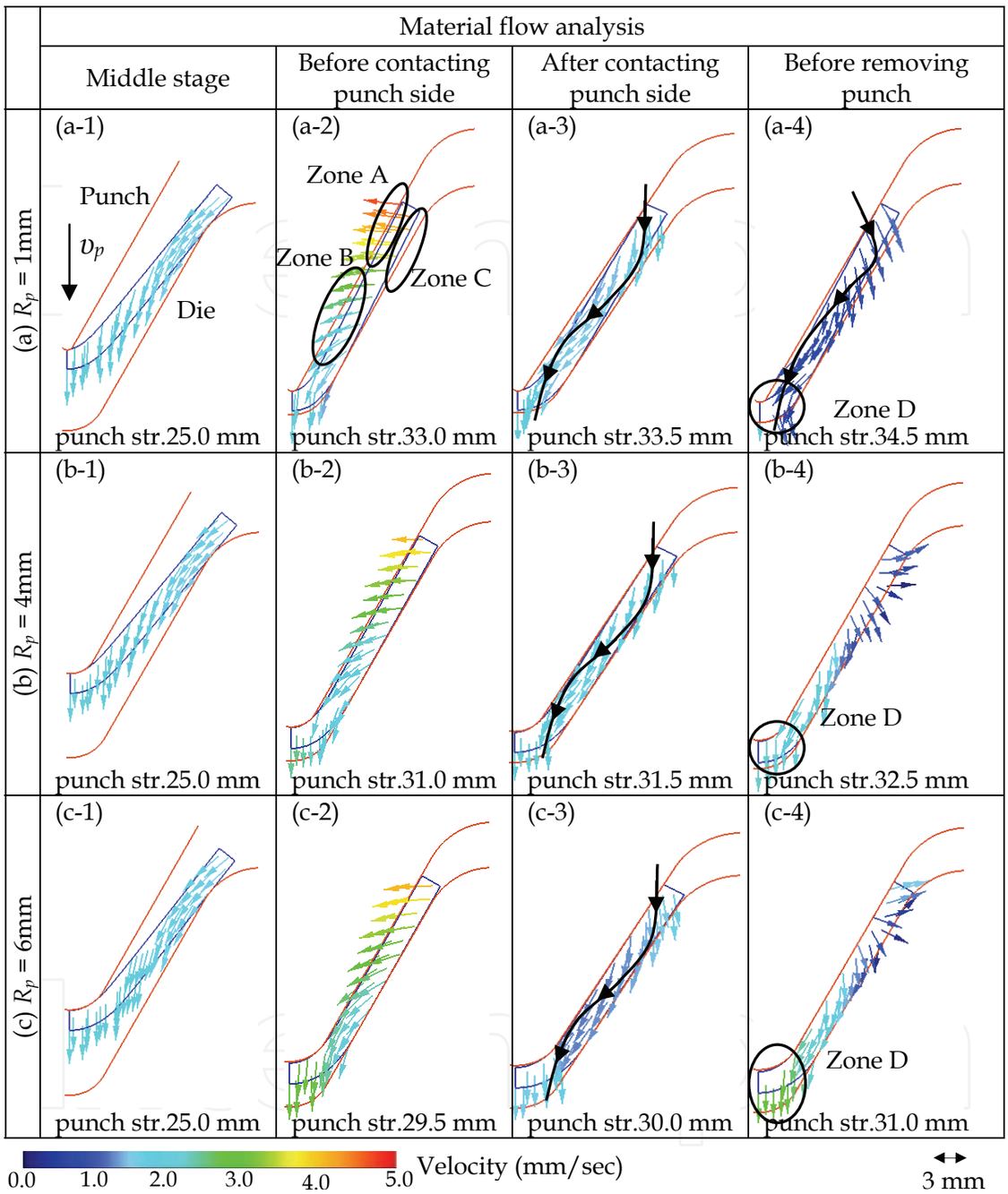

Fig. 12. Material-Flow Analysis (A1100-O, t = 3 mm, θ= 60°, R_d = 6 mm) (Thipprakmas & Rojananan, 2008)

6.2 Stress-Distribution Analysis

As mentioned in the material-flow analysis section, the material flow feature affected the stress-distribution analysis. This was also investigated and confirmed in the author's previous research (Thipprakmas & Rojananan, 2008). The FEM simulation results of the

stress distribution with reference to the punch radius are shown in Fig. 13. The stress distribution was similarly analyzed in the workpiece before the workpiece contacted the punch side, as shown in Fig. 13(a-1), (a-2), (b-1), (b-2), (c-1), and (c-2). The FEM simulation results agreed well with the bending theory (Schuler, 1998), (Lange, 1985). Specifically, tensile stress was generated on the outer surface of the workpiece, and it decreasingly propagated inward toward the neutral plane.

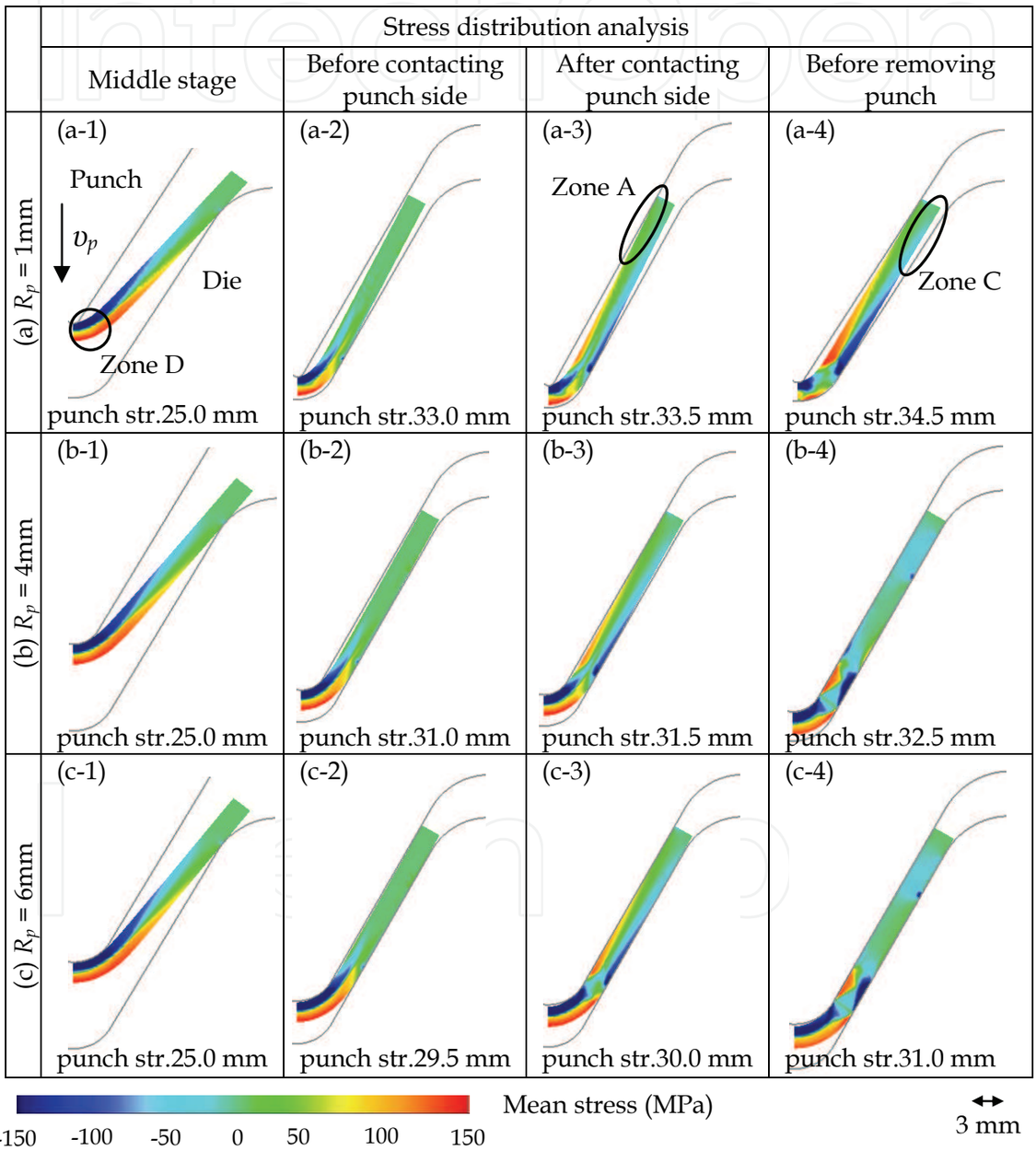

Fig. 13. Stress-Distribution Analysis (A1100-O, t = 3 mm, θ= 60°, R_d = 6 mm) (Thipprakmas & Rojananan, 2008)

Similarly, the compressive stress generated on the inner surface of the material decreasingly propagated inward toward the neutral plane. In addition, the maximum tensile and compressive stresses were generated at the zone of the bending radius, which decreasingly propagated along the leg of the workpiece. However, the bend-allowance zone increased as the punch radius increased; therefore, the analyzed stress band along the leg of the workpiece was increased as the punch radius increased. At the stage of the leg of workpiece contacting the punch side (Fig. 13(a-3), (b-3), and (c-3)), the material was pushed backward to the side of the die, resulting in an S-curve-shaped material-flow feature, in which the reverse-bending feature was generated. Specifically, tensile stress was generated on the punch side, whereas the compressive stress was generated on the die side, both of which were of reverse orientation compared with the stress distribution in the bending-radius zone. This reverse-bending feature increased as the bending stroke increased, until the end of the bending stroke. Before removing the punch (Fig. 13(a-4), (b-4), and (c-4)), the reverse-bending feature was strongly retained in the leg of the workpiece because the punch could not completely push this leg to contact the die side. This reverse bending was decreased when the punch compressed on the workpiece in the cases where the leg of the workpiece was pushed backward to contact the die side. The FEM simulation results of the stress distribution corresponded with the bending theory, and they also illustrated the correspondence with the material-flow features. The S-curve-shaped material flow resulted in the reverse bending of the leg of the workpiece. This reverse-bending feature affected the required bending angle.

6.3 Spring-back and Spring-go Characteristics

As mentioned above, due to the material-flow and stress-distribution features, the required bending angle was difficult to achieve. The stress distribution at the bend-allowance zone tried to slightly open the leg of the workpiece to the initial shape. In contrast, in the reverse-bending zone, where the tensile and compressive stresses were generated on the punch and die side, respectively, the leg of the workpiece also tried to open by the effect of the spring-back action. However, in this zone, the leg of the workpiece was reversely bent with reference to the bend–allowance zone; therefore, the leg of the workpiece tried to spring-back by slightly opening on the punch side. To predict the occurrence of spring-back or spring-go, the compensation of stress on the bend-allowance and reverse-bending zones was strictly considered. After compensating the whole stress on the workpiece, if the leg of the workpiece tried to slightly open to the punch side, it would be called “Spring-go”. This spring-go feature caused the bending angle to be smaller than the required bending angle. In contrast, if the leg of the workpiece tried to slightly open to the die side, it would be called “Spring-back”. This spring-back feature caused the bending angle to be larger than the required bending angle. This explanation was theoretically clearly described in the author’s previous research (Thipprakmas & Rojananan, 2008), and the results are shown in Fig. 14.

7. Effects of Process Parameters

In all processes, the process parameters are the most important factors that control the quality of the products and the production cost. Selection of optimized process parameters could fabricate high-quality products, in addition to reducing the production cost and time.

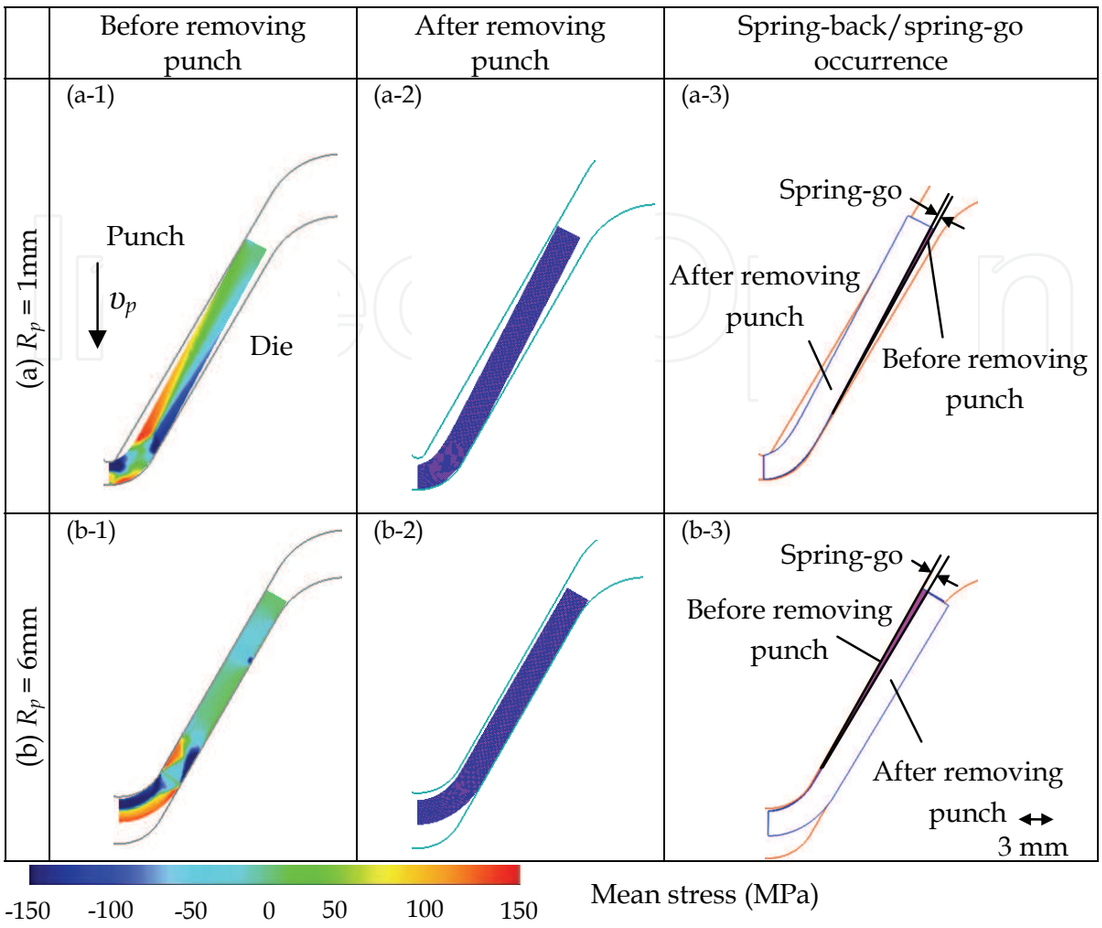

Fig. 14. Characteristics of Spring-back and Spring-go Mechanisms (A1100-O, t = 3 mm, θ= 60°, R_d = 6 mm) (Thipprakmas & Rojananan, 2008)

To prevent the occurrence of spring-back or spring-go and achieve the required bending angle in the V-die bending process, the effects of process parameters must be clearly understood. Many previous researchers studied the effects of process parameters, but most of them were aimed at the spring-back problem. Therefore, in this section, the effects of process parameters on the spring-back and spring-go effects that were investigated in the author's previous researches (Thipprakmas & Rojananan, 2008), (Thipprakmas, 2010), are clearly described. Among the investigated process parameters, the ones that mainly affect the required bending angle are the radius and height of the punch.

7.1 Punch Radius

The effects of punch radius were investigated in many previous researches and increasing the punch radius resulted in the increase of spring-back. However, in this section, the theoretical explanation of this effect will be discussed. In addition to the spring-back feature, the effects of the punch radius on the spring-go feature were also investigated and will be discussed in depth. Based on the author's previous research (Thipprakmas & Rojananan,

2008), the punch radius ranging from 1 to 6 mm was investigated. The FEM-simulation results for the spring-back and spring-go values are shown in Fig. 15. The FEM simulation results showed that the amount of spring-go decreased as the punch radius increased, whereas the amount of spring-back increased as the punch radius increased. A punch radius of 3 mm gave spring-back and spring-go values of zero; that is, the required bending angle of 60° could be achieved. To further elucidate clearly, a comparative stress-distribution analysis is shown in Fig. 16. As the punch radius increased, the bending stroke decreased because the punch pushed the leg of the workpiece backward to contact the side of the die. This process resulted in the decreasing of the reverse-bending zone. In addition, the bending zone at the punch radius increased as the punch radius increased, resulting in an increasing of the stress-distribution band and thus the amount of spring-back was increased.

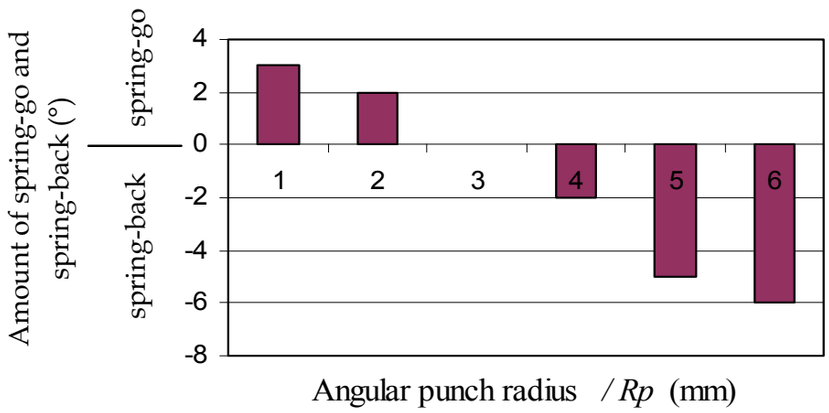

Fig. 15.The Values of Spring-back and Spring-go (A1100-O, t =3mm, θ = 60°, R_d = 6mm) (Thipprakmas & Rojananan, 2008)

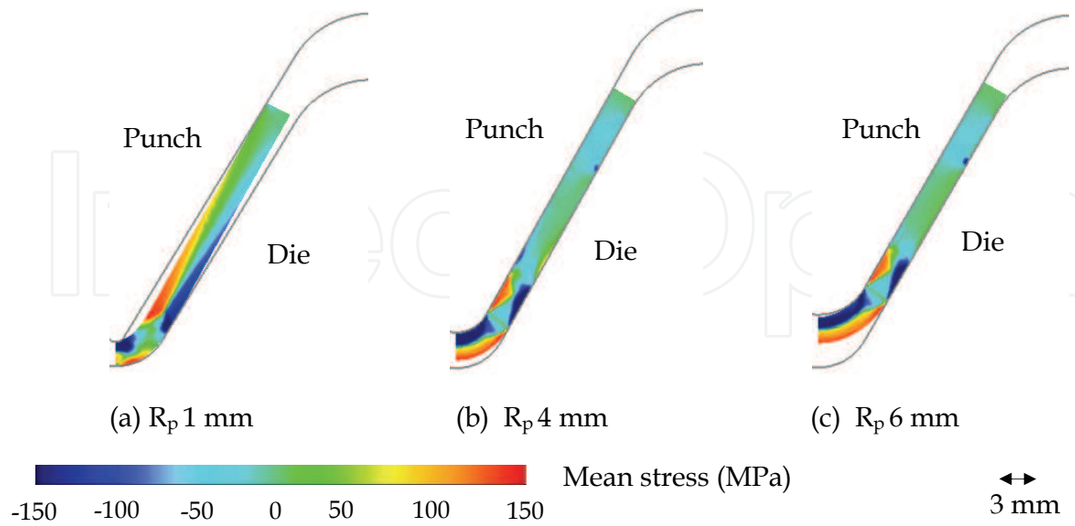

Fig. 16. Stress-Distribution Analysis with Reference to the Punch Radius (A1100-O, t =3mm, θ= 60°, R_d = 6mm) (Thipprakmas & Rojananan, 2008)

7.2 Punch Height

According to the classification of the V-die bending process mentioned above, there are two categories, as shown in Fig 6; (1) full V-die bending, and (2) partial V-die bending. The partial V-die bending uses a V-shaped punch that is smaller than the workpiece; thus, the punch cannot push the whole leg of the workpiece backward. Therefore, the punch height greatly affects the required bending angle.

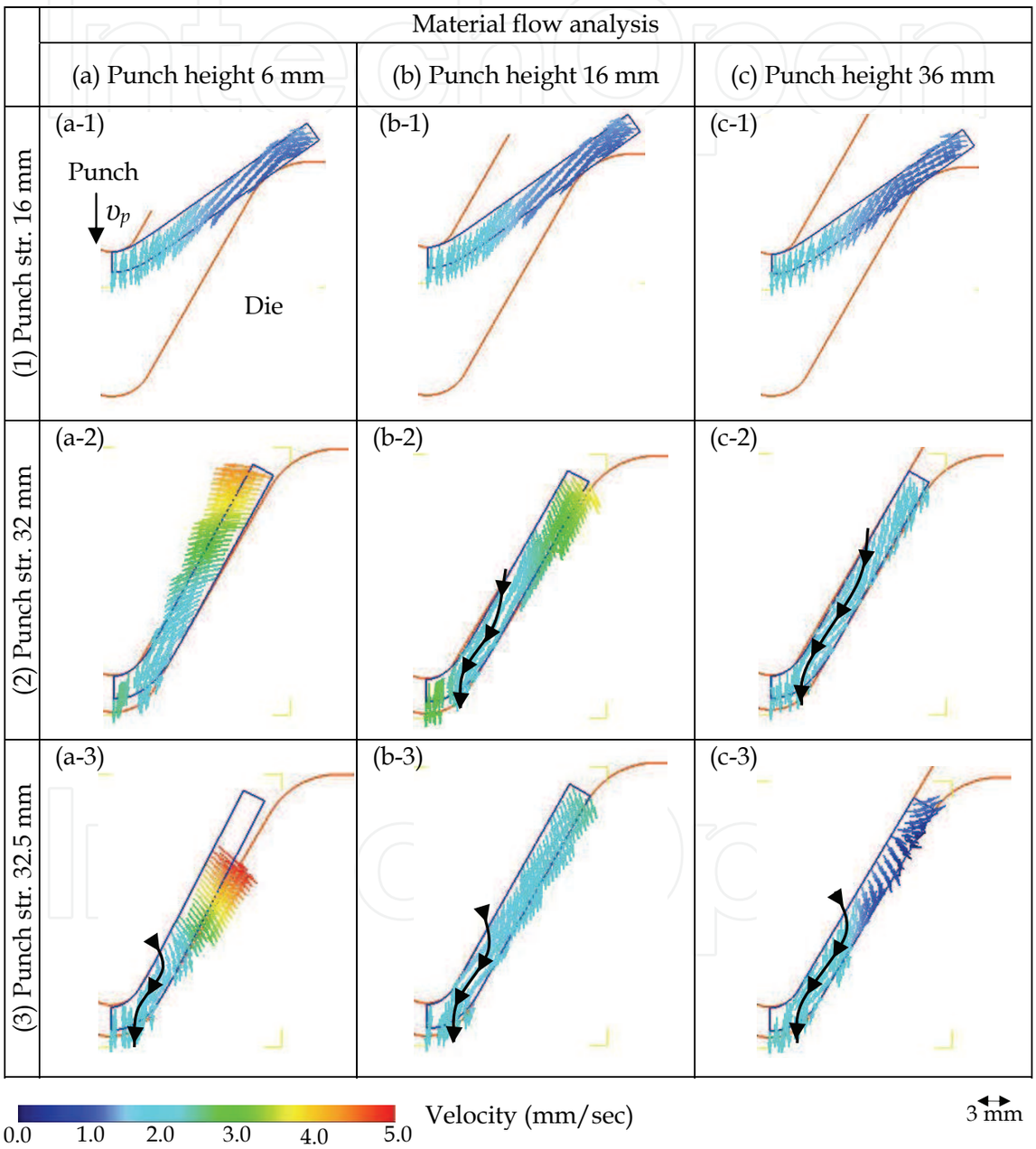

Fig. 17. Material Flow with Reference to the Punch Height (A1100-O, t =3 mm, θ= 60°, R_p = 4 mm, R_d = 6 mm) (Thipprakmas, 2010)

This effect was investigated in the author's previous research using FEM simulation and additional experiments (Thipprakmas, 2010). Fig. 17 shows the material flow in the workpiece with reference to different punch heights. Before the punch contacts the leg of the workpiece, the manner of material flow was illustrated as shown in Fig. 17(a-1), (b-1), and (c-1). With a bending stroke of approximately 32 mm, the leg of the workpiece had not yet contacted the die in the case of a punch height of 6 mm, as shown in Fig. 17(a-2). In contrast, it was pushed backward to the die side in the cases of punch heights of 16 and 36 mm, resulting in an S-curve-shaped material flow, as shown in Fig. 17(b-2) and (c-2). It was also observed that the S-curve-shaped material flow increased as the punch height increased. At the end of the bending stroke, the small height of the punch could not push the whole leg of the workpiece to contact the side of the die, resulting in a smaller bending angle. This gap between the leg of the workpiece and the die's side decreased as the punch height increased. The S-curve-shaped material flow resulted in the reverse-bending zone, with a reversed stress distribution on the leg of the workpiece.

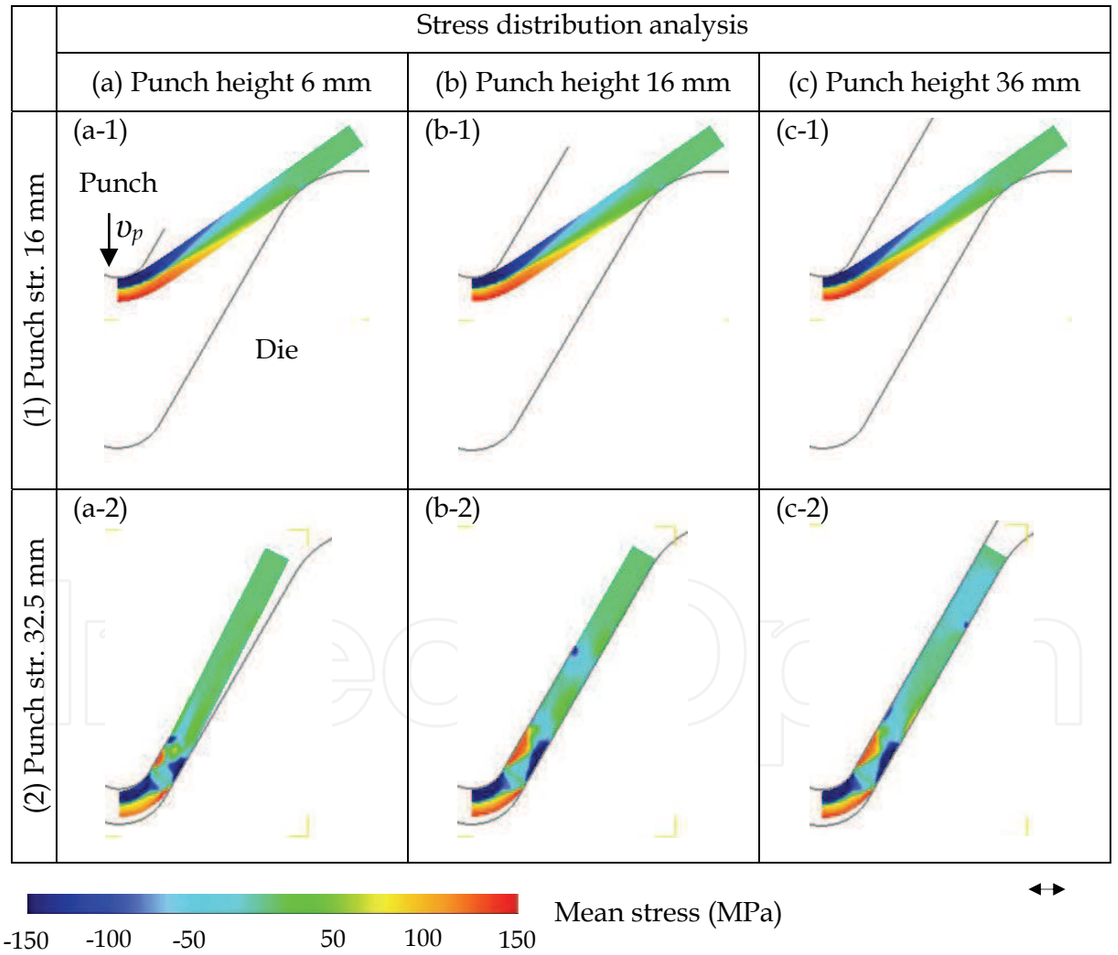

Fig. 18. Stress-Distribution Analysis with Reference to the Punch Height (A1100-O, t =3 mm, θ= 60°, R_p = 4 mm, R_d = 6 mm) (Thipprakmas, 2010)

The stress-distribution analysis with reference to the punch heights is shown in Fig. 18. Before the leg of the workpiece contacted the punch side, as shown in Fig. 18(a-1), (b-1), and (c-1), an identical manner of stress distribution was determined, which corresponded well with the bending theory. At the end of the bending stroke, Fig. 18(a-2), (b-2), and (c-2), reverse bending was generated due to the S-curve-shaped of the material flow. This reverse-bending zone was increased as the punch height increased, and it affected the required bending angle. Therefore, to achieve the required bending angle, a balance between (i) compensating the gap between the leg of the workpiece and the die side and (ii) the stress distribution on the reverse-bending zone and bend-allowance zone was strictly considered. Referring to the author's previous research (Thipprakmas, 2010), Fig. 19 shows the comparison of the bending angle with reference to the punch heights. The FEM-simulation results illustrated that the suitable punch heights to achieve the required bending angle were approximately 21 and 30 mm. The spring-go effect occurred in the cases where the punch height was smaller than 21 mm and larger than 30 mm. In contrast, the spring-back effect was observed in the case of punch heights ranging between 21 and 30 mm. As clarified above, a very small punch height caused a large gap between the leg of the workpiece and the die side, resulting in the over bending of the part. Although a small reverse bending was generated, after compensating, the bending angle obtained was smaller than the required bending angle. Vice versa, a very large punch height caused a large reverse-bending zone, which overcame the spring-back in the bend–allowance zone; therefore, the spring-go effect was generated. However, for the punch height range 21–30 mm, the reverse bending could not suppress the spring-back in the bend-allowance zone; therefore, the spring-back effect was generated.

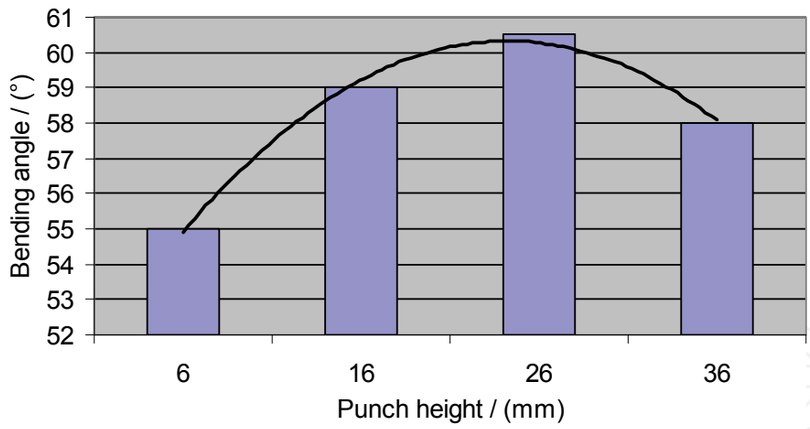

Fig. 19. Bending Angle Analyzed by FEM with Reference to the Punch Height (A1100-O, t =3 mm, θ= 60°, R_p = 4 mm, R_d = 6 mm) (Thipprakmas, 2010)

8. Validation of FEM simulation results

Laboratory experiments were carried out to validate the FEM-simulation results. Referring to the author's previous research (Thipprakmas, 2010), the experiments were carried out on an aluminum A1100-O (JIS) workpiece with the dimensions of 70-mm length, 30-mm width, and 3-mm thickness. The 5-ton universal tensile-testing machine (Lloyd Co. Ltd.) was used as the press machine. In Fig. 20, the V-bending die is shown, in addition to the tensile-

testing machine with the V-bending die set. The bending force was recorded to compare with the bending force obtained by FEM. The bending angle was measured using the profile projector. Comparing the results, the bending force and the bending angle obtained by FEM showed a good agreement with those obtained by the experiments. These results indicated that FEM simulation could be used as a tool for theoretically clarifying the mechanisms of spring-back and spring-go, in addition to studying the effects of process parameters on these effects. Furthermore, FEM can be used to predict the bending angle.

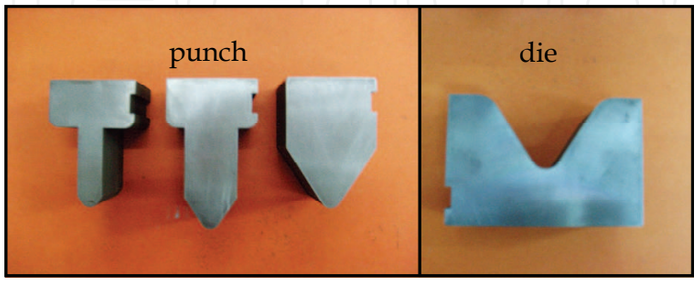

(a) V-bending punch and die

(b) V-bending die set assembled on tensile test machine

Fig. 20. The V-bending die and the Tensile-testing Machine (Thipprakmas, 2010)

8.1 Bending Force

As shown in Fig. 21, the bending forces obtained by FEM showed good agreement with those obtained by the experiments. They were somewhat constant and rapidly increased near the end of the bending stroke. This bending force corresponded well with the bending theory. However, as the punch height increased, the increase in the reverse-bending feature, resulted in an increase of the bending force.

8.2 Bending angle

The comparison of the bending angles obtained by experiments and from FEM analysis is shown in Fig. 22. The FEM-simulation results showed good agreement with the experimental results, with an error of approximately 1%.

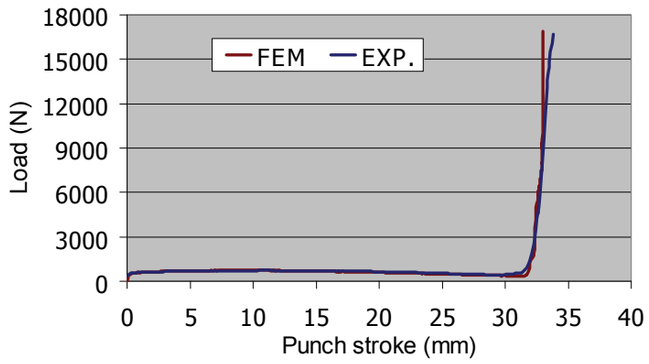

(a) Punch Height of 16 mm

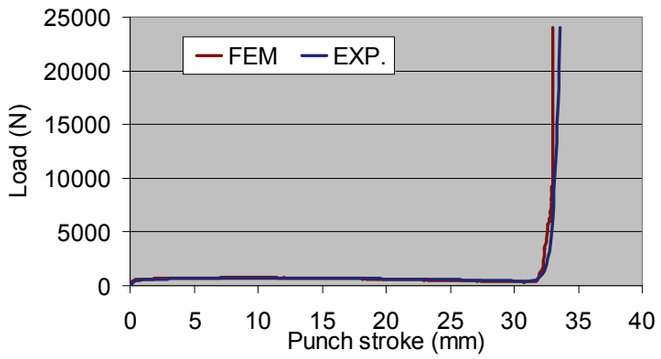

(b) Punch Height of 36 mm

Fig. 21. Comparison of the Bending Force between FEM Simulation and Experimental Results (A1100-O, t =3 mm, θ= 60°, R_p = 4 mm, R_d = 6 mm) (Thipprakmas, 2010)

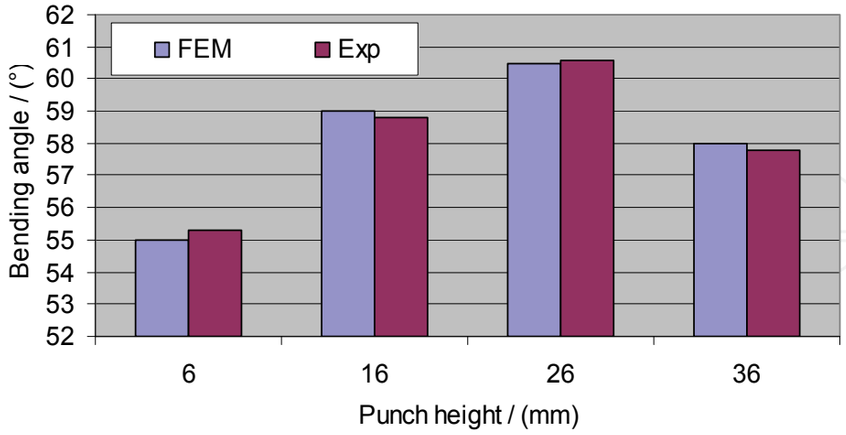

Fig. 22. Comparison of Bending Angles Obtained by FEM Simulation and Experiments (A1100-O, t =3 mm, θ= 60°, R_p = 4 mm, R_d = 6 mm) (Thipprakmas, 2010)

9. Conclusions

FEM simulation was applied to investigate the spring-back and spring-go phenomena in a V-die bending process and to investigate the effects of process parameters, including radius and height of the punch. The FEM-simulation results were validated by laboratory experiments. The FEM-simulation results showed that the spring-back and spring-go phenomena could be theoretically elucidated based on material-flow - and stress-distribution analyses. The generation of an S-curve-shaped material-flow feature caused the reversal of stress distribution on the leg of the workpiece. This reverse-stress distribution that the tensile and compressive stresses generated on the punch and die sides, respectively, resulted in a reverse-bending zone on the leg of the workpiece, and the leg of the workpiece tried to move slightly closer to the punch. After compensating the whole stress in the workpiece, the spring-go phenomenon was clearly explained when the stress generated in the reverse-bending zone overcame the stress generated in the bend-allowance zone. In contrast, the spring-back was established when the stress generated in the bend-allowance zone suppressed the stress generated in the reverse-bending zone. In addition to clearly understanding the process, the parameters affecting the spring-back and spring-go features were investigated. The FEM-simulation results illustrated that the radius and height of the punch significantly affected the spring-back and spring-go processes, in addition to the bending angle obtained. The punch radius affected the material flow. Specifically, the S-curve-shaped material flow was stronger as the punch radius decreased. This S-curve-shaped material flow resulted in reverse-stress distribution and the reverse-bending zone in the leg of the workpiece, which affected the spring-back and spring-go phenomena. The reverse-stress distribution and reverse-bending zone increased as the punch radius decreased. Therefore, the amount of spring-go decreased as the punch radius increased, whereas the amount of spring-back increased as the punch radius increased. The FEM-simulation results also illustrated that the effects of the punch height could be theoretically explained on the basis of material-flow and stress-distribution analyses. The application of a very small punch height caused a large gap formation between the leg of the workpiece and the die's side; in addition, a small reverse-bending zone was generated. In contrast, the application of a very large punch height caused a large reverse-bending zone but no gap formation between the leg of the workpiece and the die side. After compensating the whole stress distribution on the workpiece, the effect of the spring-back generated in the bend-allowance zone was not sufficient to overcome the large gap and the reverse-bending zone; therefore, the spring-go effect was generated, in which the bending angle obtained was smaller than the required bending angle in both the cases of application of very small and very large punch heights. However, if the spring-back generation on the bend-allowance zone could suppress the gap between the leg of the workpiece and the die's side, and the reverse-bending zone, spring-back was generated, in which the obtained bending angle was larger than the required bending angle. Therefore, suitable process parameters must be strictly considered to achieve the required bending angle by balancing (i) the compensation of the gap between the leg of the workpiece and the die side, and the stress distribution on the reverse-bending zone and (ii) the stress distribution on the bend-allowance zone. The FEM-simulation results were validated by laboratory experiments. The FEM-simulation results showed a good agreement with those obtained by the experiments in terms of the bending force and bending angle. These results indicated that FEM simulation could be used as a tool for the theoretical elucidation of the mechanisms of the spring-back and

spring-go phenomena, in addition to studying the effects of process parameters. Furthermore, to save production cost and time, it can be applied to industrial problems to predict the bending angle and further determine suitable process parameters.

10. References

Alexandrov, S. & Hwang, Y.M. (2009). The bending moment and spring-back in pure bending of anisotropic sheets, International Journal of Solids and Structures 46, Vol. 46, pp. 4361–4368.

Atsushi , K. & Shigeru, A. (2002). Optimized bending sequences of sheet metal bending by robot , Robotics and Computer Integrated Manufacturing, vol. 18 , pp. 29–39.

Bakhshi-Jooybari M., Rahmani B., Daeezadeh V. & Gorji A. (2009). The study of spring-back of CK67 steel sheet in V-die and U-die bending processes, Materials and Design, Vol. 30, pp. 2410-2419.

Belingardi, G. & Peroni, L. (2007). Experimental investigation of plastic collapse of aluminium extrusions in biaxial bending, International Journal of Mechanical Sciences, Vol. 49, pp. 554–566.

Canteli, J.A., Cantero, J.L. & Miguelez, M.H. (2008). Experimental identification of a thermo-mechanical model for air bending, Journal of Materials Processing Technology, Vol. 203, pp. 267–276.

Da-xin, E., Hua-hui, He., Xiao-yi, Liu. & Ru-xin, N. (2009). Spring-back deformation in tube bending, International Journal of Minerals, Metallurgy and Materials, Vol. 16, pp. 177-183.

Duflou, J.R., Vancza, J. & Aerens, R. (2005). Computer aided process planning for sheet metal bending:A state of the art, Computers in Industry 56, Vol. 56, pp. 747–771.

East, V., Darendeliler, H. & Gokler, M.I. (2002). Finite element analysis of spring-back in bending of aluminium sheets, Materials and Design, Vol. 23, pp. 223-229.

Jin, M., Thipprakmas, S., Matsumoto, N., Souma, S. & Murakawa, M. (2000). Design optimization of die and punch for bending of spring materials, Proceeding of the 51st Japaness Joint Conference for the Technology of Plasticity, pp. 481-482, Japan.

Kazan R., Firat M. & Tiryaki A.E. (2009). Prediction of spring-back in wipe-bending process of sheet metal using neural network. Materials and Design, Vol. 30, pp. 418-423.

Kim H.S. & Koc M. (2008). Numerical investigations on spring-back characteristics of aluminum sheet metal alloys in warm forming conditions, Journal of Manufacturing Processes, Vol. 204, pp. 370-383.

Lange K. Handbook of metal forming. New York: McGraw-Hill Inc.; 1985. p. 19.1-35.

Leu, D.K. & Hsieh, C.M. (2008). The influence of coining force on spring-back reduction in V-die bending process, Journal of Materials Processing Technology, Vol. 196, pp. 230–235.

Li, H., Yang, H., Zhan, M. & Kou, Y.L. (2010). Deformation behaviors of thin-walled tube in rotary draw bending under push assistant loading conditions, Journal of Materials Processing Technology, Vol. 210, pp. 143–158.

Ling, Y.E., Lee, H.P. & Cheok, B.T. (2005). Finite element analysis of spring-back in L-bending of sheet metal, Journal of Materials Processing Technology, Vol. 168, pp. 296-302.

Meinders T., Burchitz I.A., Bonte M.H.A. & Lingbeek R.A. (2008). Numerical product design: Spring-back prediction, compensation and optimization, International Journal of Machine Tool and Manufacturing, Vol. 48, pp. 499-514.

Mkaddem, A. & Saidane, D. (2007). Experimental approach and RSM procedure on the examination of spring-back in wiping-die bending processes, Journal of Materials Processing Technology, Vol. 189, pp. 325–333.

Panthi, S.K., Ramakrishnan, N., Pathak, K.K. & Chouhan, J.S. (2007). An analysis of springback in sheet metal bending using finite element method (FEM), Journal of Materials Processing Technology, Vol. 186, pp. 120-124.

Papeleux, L. & Ponthot, J.P. (2002). Finite simulation of springback in sheet metal forming, Journal of Materials Processing Technology, Vol. 25-126, pp. 785-791.

Sanchez, L.R. (2009). Modeling of spring-back, strain rate and Bauschinger effects for two-dimensional steady state cyclic flow of sheet metal subjected to bending under tension, International Journal of Mechanical Sciences, Vol. 52, pp. 429-439.

Schuler. Metal forming handbook. Berlin, Heidelberg, New York: Spring-Verlag; 1998. p. 366-373.

Tekaslan, O., Seker, U. & Ozdemir, A. (2006). Determining springback amount of steel metal has 0.5 mm thickness in bending dies, Materials and Design, Vol. 27, pp. 251-258.

Tekaslan O., Gerger N. & Seker U. (2008). Determination of spring-back of stainless steel sheet metal in ''V'' bending dies, Materials and Design, Vol. 29, pp. 1043-1050.

Thipprakmas S. & Rojananan S. (2008). Investigation of spring-go phenomenon using finite element method, Materials and Design, Vol. 29, pp. 1526-1532.

Thipprakmas S. (2010). Finite element analysis of punch height effect on V-bending angle, Materials and Design, Vol. 31, pp. 1593-1598.

Vsquez-Ojeda, C. & Ramos-Grez, J. (2009). Bending of stainless steel thin sheets by a raster scanned low power CO2 laser, Journal of Materials Processing Technology, Vol. 209, pp. 2641–2647.

Wang J., Verma S., Alexander R. & Gauc J. (2008). Spring-back control of sheet metal air bending process, Journal of Manufacturing Processes, Vol. 10, pp. 21–27.

Woznicaa, K. & Klepaczkob, J.R. (2003). Modeling of inelastic bending of a metal sheet with thermal coupling, International Journal of Mechanical Sciences 45, Vol. 45, pp. 359–372.

Yilamu, K., Hino, R., Hamasaki, H. & Yoshida, F. (2010). Air bending and spring-back of stainless steel clad aluminum sheet, Journal of Materials Processing Technology, Vol. 210, pp. 272–278.

Yu H.Y. (2009). Variation of elastic modulus during plastic deformation and its influence on spring-back, Materials and Design, Vol. 30, pp. 846-850.

Finite Element Analysis

Edited by David Moratal

ISBN 978-953-307-123-7

Hard cover, 688 pages

Publisher Sciyo

Published online 17, August, 2010

Published in print edition August, 2010

Finite element analysis is an engineering method for the numerical analysis of complex structures. This book provides a bird's eye view on this very broad matter through 27 original and innovative research studies exhibiting various investigation directions. Through its chapters the reader will have access to works related to Biomedical Engineering, Materials Engineering, Process Analysis and Civil Engineering. The text is addressed not only to researchers, but also to professional engineers, engineering lecturers and students seeking to gain a better understanding of where Finite Element Analysis stands today.

InTech Europe

University Campus STeP Ri
Slavka Krautzeka 83/A
51000 Rijeka, Croatia
Phone: +385 (51) 770 447
Fax: +385 (51) 686 166
www.intechopen.com

InTech China

Unit 405, Office Block, Hotel Equatorial Shanghai
No.65, Yan An Road (West), Shanghai, 200040, China
中国上海市延安西路65号上海国际贵都大饭店办公楼405单元
Phone: +86-21-62489820
Fax: +86-21-62489821

IntechOpen